J|A|C|S COMMUNICATIONS

Published on Web 02/10/2009

NMR Second Site Screening for Structure Determination of Ligands Bound in the Hydrophobic Pocket of HIV-1 gp41

Edina Balogh,[†] Dong Wu,[†] Guangyan Zhou,[†] and Miriam Gochin*[,†,‡]

Department of Basic Sciences, Touro University—California, Vallejo, California 94592, and Department of Pharmaceutical Chemistry, University of California, San Francisco California 94143

Received December 3, 2008; E-mail: mgochin@touro.edu

Fusion inhibitors have promising characteristics in HIV-1 prevention and therapeutics. To date, there is only one FDA-approved fusion inhibitor, the peptide T20 (Fuzeon).[1] T20 acts in a dominant negative manner, preventing the association of HIV-1 gp41 N- and C-terminal domains that accompanies fusion.[2,3] The N-terminal domain (HR1) forms a homotrimeric coiled coil, containing a hydrophobic pocket that has been identified as a hotspot for inhibiting the protein−protein interaction. It has been the target of many studies to identify low molecular weight fusion inhibitors.[4,5] However, there are no experimental details defining the orientation of small molecules in the hydrophobic pocket, since it has not been possible to crystallize the coiled coil structure in the presence of ligands other than peptides. NMR has been used to demonstrate qualitatively that small molecules bind in the hydrophobic pocket,[6] but no specific structural information has been obtained. Rational drug design for low molecular weight fusion inhibitors has therefore relied solely on computational predictions of ligand binding.[7]

We have previously described development of a stable fragment of the gp41 coiled coil that was used in a fluorescence assay to quantify small molecule binding in the hydrophobic pocket.[8] Extending these design concepts, we describe here a novel method for obtaining explicit structural constraints on a small molecule ligand bound in the hydrophobic pocket. The technique utilizes paramagnetic NMR in a second site screening approach, in which binding and orientation of the ligand is determined with respect to a second ligand (a probe) that binds with known orientation in an adjacent site. This method was first demonstrated as an NMR screening tool with the acronym SLAPSTIC, using a spin labeled probe ligand which caused strong relaxation effects on small molecules that bound in the adjacent site.[9] It was recognized that differential paramagnetic relaxation effects (PREs) could potentially be used to determine the alignment between the two ligands.[10] Transferred pseudocontact shifts (PCSs) have also been demonstrated in the determination of ligand binding using lanthanide substitution in an instrinsic metal-binding site.[11]

The SLAPSTIC and transferred PCS effects were applied to the study of low affinity ligands in fast exchange, for which substantial scaling of the paramagnetic effect occurs. This prevents excessive broadening or shifting of ligand resonances and permits detection through resonances of the free ligand. SLAPSTIC has not been demonstrated as a quantitative structural tool, possibly because the paramagnetic component of ligand relaxation can be difficult to obtain accurately, requiring measurement of exactly matched diamagnetic and paramagnetic samples, and incurring additive experimental errors when taking the difference of two proton relaxation rates. The approach that we describe here overcomes some of the limitations in adapting the methodology to structure determination of bound ligands. Our method does not require ligands to be in fast exchange or perfectly matched paramagnetic and diamagnetic samples. Instead the PCS and PRE effects are modulated by varying the fraction of bound probe, and the diamagnetic component can be accurately extracted as a function of fractional occupancy of the ligand. Furthermore, we use as a probe a segment of the C-terminal domain helix of gp41, which not only has a well-defined structure but also stabilizes the inherently hydrophobic coiled coil in solution, preventing aggregation.[12] Application to gp41 presents a unique opportunity to characterize small molecule binding to the hydrophobic pocket and offers a technique that can be generalized to the study of inhibitors of protein−protein interactions.

A key feature of our system is the design of a stabilized extended gp41 coiled coil structure in solution, to use as a receptor for both probe peptide and ligand binding. We have developed a 45-residue long bipyridylated HR1 segment env5.0 (bpy-GQAVSGIVQQQ-NNLLRAIEAQQHLLQLTVWGIKQLQARILAVEKK-NH_2), which forms a coiled coil structure upon addition of 1/3 stoichiometry of ferrous ions. We have demonstrated nanomolar binding of a 39-residue cognate C-peptide to this construct (manuscript in preparation). For this application, we have designed a truncated C-peptide, C29-e5.0 (Ac-CYTSLIESLIRESQEQQEKNEQELRELDK-NH_2), which is missing the hydrophobic pocket-binding residues. It has an N-terminal cysteine positioned at the edge of the pocket and pointing away from the protein−protein interaction surface. Labeling with a paramagnetic reporting group provides a system sensitive to ligand binding in the pocket. The concept is illustrated in Figure 1. The cysteine is labeled with the spin label MTSL or with cysteaminyl-EDTA (Toronto Research Chemicals). Distance and orientation dependent changes in ligand resonances are induced upon binding, providing positional constraints on bound ligand conformation.

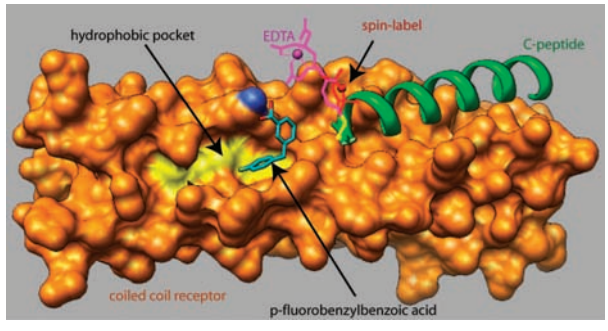

Figure 1. Model demonstrating second site screening for the hydrophobic pocket. A spin label or EDTA moiety is attached to an outer C-peptide (green) which binds in a site adjacent to the pocket. The coiled coil is shown as an orange surface with the floor of the pocket emphasized in yellow. The small ligand p-fluorobenzylbenzoic acid is shown docked in a pose which agrees with the NMR data (see text).

[†] Touro University—California.
[‡] University of California.

10.1021/ja8094558 CCC: $40.75

We demonstrate this experiment using a low affinity ligand, 3-*p*-fluorobenzylbenzoic acid (3p-FB), which binds to the hydrophobic pocket with a $K_I = 0.55 \pm 0.05$ mM. This molecule was developed as a highly soluble fragment of the hydrophobic pocket binder 11{6,11}.[8] Line broadening of 3p-FB occurs upon addition of 4% Fe(env5.0)$_3$ (data not shown), confirming both ligand binding and the accessibility of the hydrophobic pocket. C29-e5.0 binds to Fe(env5.0)$_3$ with a 3 ± 0.33 μM K_I. Ligand and probe peptide binding constants were determined using our competitive inhibition fluorescence assay[8] (Supporting Information). Figure 2 shows the

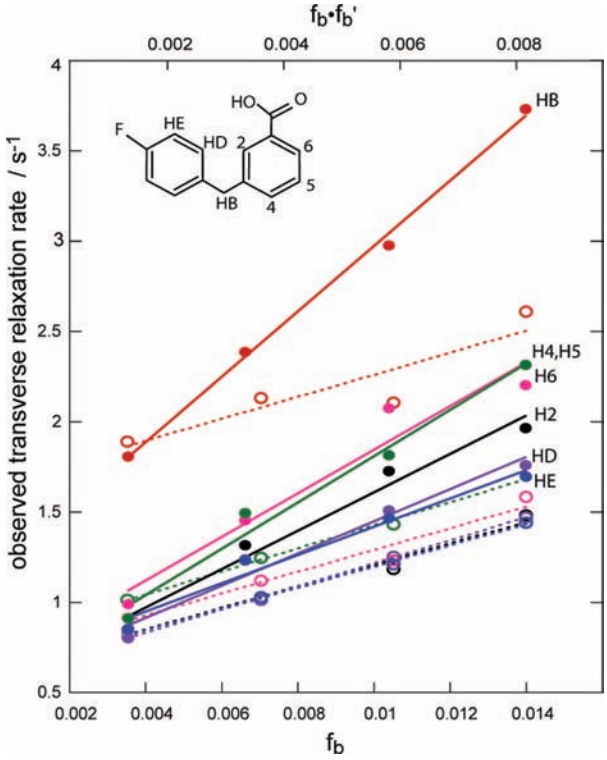

Figure 2. Plot of relaxation rates of 300 μM 3p-FB (shown inset) with Fe(env5.0)$_3$ and unlabeled or MTSL-labeled C29-e5.0 in ratios of 3:3, 6:6, 9:9, 12:12 μM. Relaxation rates in the diamagnetic sample are plotted against f_b (open symbols and dashed lines); relaxation rates in the paramagnetic sample are plotted against $f_b \cdot f_b'$ (closed symbols, solid lines). Experiments were conducted at 500 MHz. Protons H4 and H5 are overlapping.

observed transverse relaxation rates of 300 μM 3p-FB in the presence of increasing amounts of Fe(env5.0)$_3$ and C29-e5.0. The amounts of receptor and probe peptide were kept equal to avoid any aggregation of the receptor. Two data sets were obtained for unlabeled and MTSL-labeled C29-e5.0. Clear differentiation between the diamagnetic and paramagnetic relaxation rates was observed. Diamagnetic relaxation as a function of the fraction of bound ligand, f_b, could be fit to a straight line, in accordance with the expected dependence of the observed relaxation rate R_{2obs}^{dia} in a fast-exchanging system:

$$R_{2obs}^{dia} = f_b(R_{2b}^{dia} - R_{2f} + R_2^{ex}) + R_{2f} \quad (1)$$

R_{2f} and R_{2b}^{dia} are the transverse relaxation rates of free ligand and ligand bound in the presence of diamagnetic probe peptide, respectively. R_2^{ex} is an exchange broadening term. ($R_{2b}^{dia} - R_{2f} + R_2^{ex}$), obtained from the slope of the fit to eq 1, varies by less than 4% between the different ligand protons.

The observed paramagnetic relaxation R_{2obs}^{para} depends on the product of f_b with f_b', the fractional occupancy of the probe, according to

$$R_{2obs}^{para} = f_b \cdot f_b' \cdot R_{2b}^{para} + R_{2obs}^{dia} \quad (2)$$

Subtraction of the diamagnetic best-fit line from the paramagnetic data will give a straight line with slope R_{2b}^{para} when plotted against $f_b \cdot f_b'$. R_{2b}^{para} is directly related to the inverse sixth power of the distance from spin label to observed proton, according to the Solomon−Bloembergen equations.[13] It varies by more than 200% among protons of the ligand, indicating a system highly sensitive to proton position with respect to the spin label.

Importantly, measurement at various receptor and probe peptide concentrations allows for averaging of the errors associated with measuring individual data points. In fact in this case, where diamagnetic slopes are essentially equal for all protons, a single diamagnetic condition prevails for the whole ligand. Additionally, the diamagnetic samples do not need to have exactly the same composition as the paramagnetic samples to obtain the trendlines.

A second experiment illustrating PCS effects is shown in Figure 3, using EDTA-labeled C29-e5.0 either free or complexed to Co^{2+}.

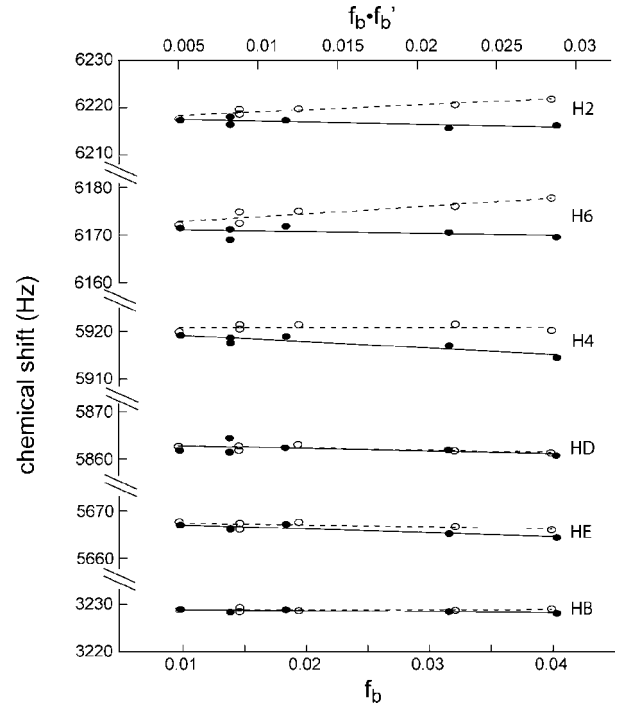

Figure 3. Observed chemical shifts of 50 μM 3p-FB in the presence of Fe(env5.0)$_3$: EDTA-C29-e5.0 in ratios of 6:6, 9:9, 12:12, 20:20, and 25:25. Data were obtained in the absence (plotted against f_b, open symbols and dashed lines) and in the presence of Co^{2+} (plotted against $f_b \cdot f_b'$, closed symbols and solid lines). Experiments were performed at 800 MHz.

Clear differentiation in chemical shift behavior was observed as a function of proton position, the PCS effect depending not only on distance from the spin label but also on orientation. For example, HB protons of the methylene group experienced the largest paramagnetic relaxation effect, but a very small pseudocontact shift. This indicates that the positive and negative lobes of the Co^{2+} magnetic susceptibility anisotropy tensor intersect close to HB, a result that can be used to help define the tensor orientation. Similar equations to eqs 1 and 2 hold for the variation of ligand shifts with f_b and f_b', except for the absence of the exchange term of eq 1. As with the paramagnetic relaxation effect, the slope of the paramagnetic data minus the diamagnetic trendline gives the pseudocontact shift of bound ligand protons, which is a global structural constraint on their position.[14,15] Averaging of several experiments is once

again advantageous in reducing error, especially in the case of a weakly binding ligand where the residual shifts are small, as in this case.

This method relies on precise determination of ligand and probe binding constants. The experimental error in the K_D's translates into a 10% error in R_{2b}^{para} or δ_{PCS}. These errors should be included in structure calculations. An inaccuracy in f_b' can be absorbed by the scaling factors (spectral density or susceptibility tensor magnitudes) linking R_{2b}^{para} or δ_{PCS} to the structural constraints. Thus a system can be calibrated for a given peptide probe without requiring accurate determination of peptide K_D. For universal application involving multiple probe peptides, accuracy in peptide K_D's is required.

Cross-validation of low energy docked conformations and minimization with the PRE data yielded the unique pose of 3p-FB shown in Figure 1. The carboxylate group makes a hydrogen bond with a pocket lysine residue, in common with a similar effect observed for the C-peptide bound in the pocket. The methylene group HB and the edge of the ring supporting protons H4 and H5 are closest to the labeled probe peptide. We obtained an excellent fit between observed and calculated PCS data for this ligand conformation, by allowing variation of tensor parameters. This was not possible using non-PRE-minimized docked conformations (Supporting Information).

Structural information is critical for rational design of more potent inhibitors. In a separate study, we will apply PRE and PCS restrained molecular dynamics simulations for a more detailed structure determination of the bound ligand, taking into account the flexibility of the paramagnetic reporter groups[16] and PREs from both the spin label and a Mn^{2+}−EDTA system.

It is relatively easy to modulate the affinity of the C-peptide for the gp41 receptor and therefore to change the amplitude of PRE and PCS effects. Mutations of residues involved in groove binding or in helical propensity have been shown to sensitively affect the peptide affinity.[17−19] By studying low affinity ligands with a strongly binding probe peptide and high affinity ligands with a weakly binding probe peptide, we can always obtain a weighted average of the paramagnetic effect, scaled according to fractional occupancy (see Supporting Information for additional discussion). This tuning is not possible if the protein receptor is labeled directly. In slow exchange, protein resonances in the pocket can also be characterized, with isotopic labeling to distinguish between resonances of the protein and ligand. The use of a paramagnetically labeled probe peptide rather than direct labeling of the receptor not only enables tuning and accurate determination of PRE and PCS, as shown above, but also avoids peak doubling of receptor resonances in PCS measurements, a common problem associated with stereoisomerization of metal−EDTA coordination.[20]

In conclusion, we have demonstrated a unique method for structural characterization of a ligand bound in the hydrophobic pocket of gp41. This is the first explicit definition of a low molecular weight inhibitor of gp41, providing a significant advance in methodology for structure-based drug design of nonpeptide fusion inhibitors. The method can be applied to other viruses with a similar fusion mechanism to HIV and potentially to a variety of protein−protein interaction targets.

Acknowledgment. This work was supported by NIH Grant NS059403 to M.G. Molecular graphics images were produced using the UCSF Chimera package from the Resource for Biocomputing, Visualization, and Informatics at the University of California, San Francisco (supported by NIH P41 RR-01081). The authors thank Dr. Lifeng Cai for assistance with determination of the ligand inhibition constant, Dr. Jeff de Ropp at the UC Davis NMR facility for access and help with use of the NMR facility, and Dr. Robert Rizzo at SUNY Stonybrook for providing receptor and initial docked ligand coordinates.

Supporting Information Available: Binding data, PCS fitting, and notes on ligand exchange rates. This material is available free of charge via the Internet at http://pubs.acs.org.

References

(1) Greenberg, M. L.; Cammack, N. *J. Antimicrob. Chemother.* **2004**, *54*, 333–40.
(2) Wexler-Cohen, Y.; Johnson, B. T.; Puri, A.; Blumenthal, R.; Shai, Y. *J. Biol. Chem.* **2006**, *281*, 9005–10.
(3) Eckert, D. M.; Kim, P. S. *Annu. Rev. Biochem.* **2001**, *70*, 777–810.
(4) Eckert, D. M.; Malashkevich, V. N.; Hong, L. H.; Carr, P. A.; Kim, P. S. *Cell* **1999**, *99*, 103–15.
(5) Liu, S.; Wu, S.; Jiang, S. *Curr. Pharm. Des.* **2007**, *13*, 143–62.
(6) Frey, G.; Rits-Volloch, S.; Zhang, X. Q.; Schooley, R. T.; Chen, B.; Harrison, S. C. *Proc. Natl. Acad. Sci. U.S.A.* **2006**, *103*, 13938–43.
(7) Teixeira, C.; Barbault, F.; Rebehmed, J.; Liu, K.; Xie, L.; Lu, H.; Jiang, S.; Fan, B.; Maurel, F. *Bioorg. Med. Chem.* **2008**, *16*, 3039–48.
(8) Cai, L.; Gochin, M. *Antimicrob. Agents Chemother.* **2007**, *51*, 2388–95.
(9) Jahnke, W.; Perez, L. B.; Paris, C. G.; Strauss, A.; Fendrich, G.; Nalin, C. M. *J. Am. Chem. Soc.* **2000**, *122*, 7394–5.
(10) Jahnke, W. In *BioNMR in Drug Research*; Zerbe, O., Ed.; Wiley-VCH: Weinheim, 2003; pp 341−354.
(11) John, M.; Pintacuda, G.; Park, A. Y.; Dixon, N. E.; Otting, G. *J. Am. Chem. Soc.* **2006**, *128*, 12910–6.
(12) Weissenhorn, W.; Calder, L. J.; Dessen, A.; Laue, T.; Skehel, J. J.; Wiley, D. C. *Proc. Natl. Acad. Sci. U.S.A.* **1997**, *94*, 6065–9.
(13) Solomon, I.; Bloembergen, N. *J. Am. Chem. Soc.* **1956**, *25*, 261–266.
(14) Bertini, I.; Luchinat, C. *NMR of Paramagnetic Molecules in Biological Systems*; Benjamin/Cummins Publishing Co. Inc.: 1986; Vol. 3.
(15) Tu, K.; Gochin, M. *J. Am. Chem. Soc.* **1999**, *121*, 9276–85.
(16) Iwahara, J.; Schwieters, C. D.; Clore, G. M. *J. Am. Chem. Soc.* **2004**, *126*, 5879–96.
(17) Dwyer, J. J.; Wilson, K. L.; Davison, D. K.; Freel, S. A.; Seedorff, J. E.; Wring, S. A.; Tvermoes, N. A.; Matthews, T. J.; Greenberg, M. L.; Delmedico, M. K. *Proc. Natl. Acad. Sci. U.S.A.* **2007**, *104*, 12772–7.
(18) Wang, S.; York, J.; Shu, W.; Stoller, M. O.; Nunberg, J. H.; Lu, M. *Biochemistry* **2002**, *41*, 7283–92.
(19) Otaka, A.; Nakamura, M.; Daisuke, N.; Kodama, E.; Uchiyama, S.; Nakamura, H.; Kobayashi, Y.; Matsuoka, M.; Fujii, N. *Angew. Chem., Int. Ed.* **2002**, *41*, 2938–9.
(20) Ikegami, T.; Verdier, L.; Sakhaii, P.; Grimme, S.; Pescatore, B.; Saxena, K.; Fiebig, K. M.; Griesinger, C. *J. Biomol. NMR* **2004**, *29*, 339–49.

JA8094558